Metawaveguide for Asymmetric Interferometric Light-Light Switching

Han Zhao, William S. Fegadolli, Jiakai Yu, Zhifeng Zhang, Li Ge, Axel Scherer, and Liang Feng

Phys. Rev. Lett. **117**, 193901 — Published 31 October 2016

DOI: 10.1103/PhysRevLett.117.193901

Metawaveguide for Asymmetric Interferometric Light-Light Switching

Han Zhao[1†], William S. Fegadolli[2†], Jiakai Yu[1†], Zhifeng Zhang[1], Li Ge[3], Axel Scherer[2] and Liang Feng[1*]

[1]*Department of Electrical Engineering, The State University of New York at Buffalo, Buffalo, NY 14260, USA*

[2]*Department of Physics and Kavli Nanoscience Institute, California Institute of Technology, Pasadena, CA 91125, USA*

[3]*Department of Engineering Science and Physics, College of Staten Island, CUNY, Staten Island, NY 10314, USA and The Graduate Center, CUNY, New York, NY 10016, USA*

[†]These authors contributed equally to this work.

*Email: fengl@buffalo.edu

Light-light switching typically requires strong nonlinearity where intense laser fields route and direct data flows of weak power, leading to a high power consumption that limits its practical use. Here we report an experimental demonstration of a metawaveguide that operates exactly in the opposite way in a linear regime, where an intense laser field is interferemetrically manipulated on-demand by a weak control beam with a modulation extinction ratio up to approximately 60 dB. This asymmetric control results from operating near an exceptional point of the scattering matrix, which gives rise to intrinsic asymmetric reflections of the metawaveguide through delicate interplay between index and absorption. The designed metawaveguide promises low-power interferometric light-light switching for next generation of optical devices and networks.

PACS: 42.79.-e, 42.25.Bs, 78.67.Pt

Effective light-light switching promises optical information processing, which has been a longstanding driving force for high-speed and energy-efficient optical networks. Strong optical modulations are initiated in nonlinear optical media by intense laser fields to enable switching of a weak signal, for example, intensity modulation of light by light has been demonstrated based on the all-optical Kerr effect [1-6]. Nevertheless, the high power requirement for the intense control/pump light becomes a significant barrier for practical applications. While cavity quantum electrodynamics displays nonlinear optical effects on a few-photon level [7,8], its application as a robust optical element operating in the classical regime remains still unclear. On the other hand, a recent pioneering investigation of exploiting photonics absorption offered a unique linear scheme to efficiently control light by light utilizing mutually coherent interaction of light beams and absorbing matters [9,10], by which coherent perfect absorption (CPA) was demonstrated [11-14]. While this linear strategy reduces the power requirement, the control beam still has a similar amount of power as the actual source signal in these previous works, due to the rather symmetric optical scatterings in the optical implementations.

The recent emergence of non-Hermitian photonic metamaterials offers a new paradigm to explore nanophotonics and metamaterials research in the entire complex dielectric permittivity plane, based on parity-time (PT) symmetry [15-20]. Attractive physical phenomena including phase transitions and exceptional points are emulated with photonics, consequently leading to novel effective manipulation of cavity lasing modes [21-26] and unidirectional light transport [27-32]. Here, we will show a unique metawaveguide of potential for on-demand control of interferometric light-light switching can be realized through non-Hermitian metamaterial explorations.

An intriguing characteristic of non-Hermitian photonic metamaterials is their intrinsic asymmetry near an exceptional point. For PT symmetric systems in particular, these exceptional points can either represent asymmetric transmission resonances [27-30] or a violation of energy conservation in the scattering eigenstates, depending on the formulation of the scattering matrix [30]. Here, we delicately design the interplay between index and absorption to construct a metawaveguide by exploring the former type of exceptional points. An asymmetry in reflection arises near the exceptional point and is further utilized to facilitate asymmetric light-light switching in a linear regime, where a weak control beam can be interferometrically exploited to control an intense laser signal, resulting in two distinct modes of operation, i.e., CPA or strong scattering. The experimental results show the metawaveguide enables low-power interferometric weak-intense light-light control of an extinction ratio up to approximately 60 dB, promising highly-efficient integrated photonic switches for data guiding, routing and switching around optical communication networks.

The optical transfer matrix describes the related scattering eigenstates of an optical system. For a two-port system of length L, a transfer matrix M links the scattering eigenstates of both ports as

$$\begin{pmatrix} A(L) \\ B(L) \end{pmatrix} = \begin{pmatrix} M_{11} & M_{12} \\ M_{21} & M_{22} \end{pmatrix} \begin{pmatrix} A(0) \\ B(0) \end{pmatrix}, \tag{1}$$

where $A(0)$ and $B(L)$ are inputs in left and right ports, while $B(0)$ and $A(L)$ denote outputs in left and right ports, respectively. To facilitate interference-enhanced absroption for switching, the CPA condition $M_{11}=0$ is desired, which corresponds to input light being completely absorbed [10,11,21]. The goal we set to achieve, i.e., using a weak control beam $B(L)$ to bring a strong signal beam $A(0)$ into CPA, is satisfied when $|M_{21}| << 1$, which corresponds to a strongly *asymmetric reflection*, i.e., $|r_L| \ll |r_R|$ [33]. This condition requires a non-Hermitian system since reciprocity of light propagation in a Hermitian system implies $|r_L| = |r_R|$. Here to create an asymmetry in light reflection, we take the approach inspired by asymmetric transmission resonances [27-30] in a PT symmetric metawaveguide. More specifically, we manipulate the spatial index-absorption modulation of the metawaveguide in the vicinity of the exceptional point, i.e. the quasi-PT symmetry phase transition point where $r_L = 0 << |r_R|$, satisfying the requirement of asymmetric reflection mentioned above.

Fig. 1(a) shows the schematic on a silicon-on-insulator (SOI) platform. The metawaveguide is designed to be 800 nm wide and 220 nm thick, embedded in a background of SiO_2, supporting a fundamental mode with an effective wavenumber of $k_1 = 2.69k_0$ at the wavelength of 1550 nm, where k_0 is the wavenumber in free space. The non-Hermitian optical potential is enforced along the length of the metawaveguide with the index-absorption engineering, and reads

$$\Delta\varepsilon = \Delta\varepsilon_0 \left(\cos(qz) + i\delta \sin(qz)\right), \tag{2}$$

where $\Delta\varepsilon_0 = 0.317$ denotes the modulation amplitude, δ is larger than 1 ($\delta = 1$ corresponds to the exceptional point [27-29]) to have the device operating in the symmetry breaking phase, and $q = 2k_1$, and the modulation regions are located at $4n\pi/q \le z \le 4n\pi/q + \pi/q$ (n=1, 2, 3…). Due to the coupling between forward and backward propagating light by the modulated dielectric constant, the metawaveguide supports two degenerate Bragg modes of different absorption coefficients. To maximize the extinction ratio for switching in the device, the length of the device is designed to be approximately 21.9 μm corresponding to 38 periods [33], such that one degenerate mode satisfies the CPA condition, i.e. $M_{11} = 0$, where coherent light inputs from the left and right ports are perfectly absorbed with zero output scatterings (see Fig. 1(b); upper panel). The other degenerate mode has much less absorption and thus generates strong output scatterings (see Fig. 1(b); lower panel). Assuming the incident phase of the signal remains 0, efficient switching between these two modes of operation can be achieved by tuning the incident phase of the control field from π/2 to –π/2, with an extremely remarkable extinction ratio.

The interferometric light-light switching is facilitated by the asymmetric reflection of the designed metawaveguide attributed to the exceptional point. However, operating too close to the exceptional point leads to a low transmission efficiency [33] and is also challenging in fabrication. Here a relatively small value of $\delta = 2$ was chosen to obtain a reasonable transmission efficiency and ensure that fabrication imperfections do not make the system deviate strongly from the designed CPA condition. We find that the intensity ratio ξ is given by $(\delta+1)/(\delta-1)$, leading to ξ of 3:1 between the strong signal beam and the weak control beam [33], which is in contrast to the previous approaches of controlling light with light using both linear and nonlinear strategies [1-14].

To demonstrate the metawaveguide with the desired intrinsic scattering asymmetry, an equivalent guided-mode modulation has been designed to realize the virtual non-Hermitian function modulation with in-phase separation of real index and imaginary absorption modulations, as illustrated in Fig. 2(a). The equivalence to the original quasi-PT modulation was validated by the consistent mode effective indices of guided light for both real index and imaginary absorption modulations, respectively, enabling the same asymmetric reflection. The sample was then fabricated using overlay electron beam lithography, followed by electron beam evaporation and lift-off of sinusoidal shaped Cr/Ge combos and dry etching to form the Si waveguide with cosine shaped side wall modulations, respectively [33]. The pictures of the metawaveguide before deposition of SiO_2 as top cladding are shown in Figs. 2(b) and 2(c).

In our experiments, coherent laser beams, splitted from the same laser source, were coupled from free space to tapered polarization-maintaining fibers to deliver light into the waveguide from both ports, by means of specifically designed mode converters. The experimental validation of the asymmetric interferometric light-light switching required precise measurements of the ratio of outputs to inputs consisting of both reflection and transmission. We implemented two on-chip waveguide directional couplers to separate the inputs and outputs and route them to 4 respective grating couplers [Fig. 3(a)]. The grating couplers efficiently scattered input and output light to free space, which was collected by a microscope objective and further imaged onto a highly sensitive charge-coupled device (CCD) camara for final evalutions [33]. As a result, the output scattering coefficient from the device was characterized by

$$Q_s = 10\log\left[(O_1+O_2)/(I_1+I_2)\right]+C, \tag{3}$$

where O_1 and O_2 are scattered light from two output grating couplers, I_1 and I_2 are scattered light from two input grating couplers, and C is a constant denoting the overall detection loss to the output scatterings by the directional couplers. The incident phase of the control field was well controlled by an optical delay line constructed in free space. The intensity ratio ξ of the signal beam to the control beam was manipulated to the designed value of 3 (corresponding to $\delta = 2$) by adjusting the coupling efficiency of the control beam, confirmed by imaging the scattered light from the corresponding input grating couplers. The spectra of the output scatterings of the fabricated non-Hermitian waveguide have been measured for both minimum and maximum Q_s, corresponding to the CPA mode and the other degenerate mode of less absorption, respectively, as shown in Fig. 3(b). At the resonant wavelength of the non-Hermitian waveguide, the CPA mode was achieved with almost no output scatterings when the incoming phase of the control was φ = π/2, as shown in the lower panel inset of Fig. 3(b). In contrast, the mode of less absorption was excited and strong outputs were observed when the phase of the control was modulated to φ = -π/2 [upper panel inset of Fig. 3(b)], demonstrating a weak-to-intense optical switching with an extinction ratio up to approximately 60 dB in the metawaveguide.

Because the metawaveguide was operated in the vicinity of the exceptional point, such asymmetric interferometric light-light switching in output scatterings remained as a function of wavelength detuning Δ [Fig. 3(b)]. However, the phase response of output scatterings was different if moving away from the resonance. At the resonant wavelength, i.e. $\Delta = 0$, two output grating couplers manifested consistently in-phase on/off light scatterings for O_1 and O_2 in spite of interferometic control [Fig. 4(a)], whereras if $\Delta \neq 0$, output light scatterings became out-of-phase as different on/off relations were observed for O_1 and O_2 [Figs. 4(b)-4(c)]. This was because an additional phase shift was inherently associated with the Floquet-Bloch periodic boundaries due to the periodic nature of the modulation in the waveguide. Moreover, the Floquet-Bloch periodic boundaries caused the sign of the phase shift reversed if the operating wavelength crossed over the boundary of the Brillouin zone. Hence, output light scatterings showed opposite out-of-phase on/off responses with respect to interferometic control of the control at $\Delta < 0$ [Figs. 4(b)] and $\Delta > 0$ [Figs. 4(c)].

The asymmetric interferometric light-light switching we have accomplished utilizing a non-Hermitian metawaveguide promises new approaches to optical information processing. Operating in the vicinity of an exceptional point, the metawaveguide allows a weak control light field to strongly modulate the outputs of a large optical source signal through interference-enhanced absorption. Interferometric control of the weak control beam demonstrates light switching in output scatterings with an extinction ratio of approximately 60 dB. In principle, the control power can be further engineered to be much weaker than the signal power by reducing the modulation depth δ of $\mathrm{Im}[\Delta\varepsilon]$ responsible for the asymmetric reflection. Although the proposed metawaveguide does not break Lorentz reciprocity, further consideration with nonlinearity [34] may promise novel optical isolators [35] and highly integrated all-optical transistors gates [36]. Integration of Kerr nonlinearity may also enable an approach to flexibly manipulate the metawaveguide towards or away from the EP [37], proving an additional freedom in the interferometric light-light switching. This interferometric light-light switching effect may be enhanced if the material absorption is further magnified using optical metamaterials [38].

Acknowledgement

The work is supported by US Army Research Office (W911NF-15-1-0152) and National Science Foundation (DMR-1506884). L.G. acknowledges the support by National Science Foundation (DMR-1506987). W.S.F. and A.S. acknowledge Boeing for their support under their SRDMA program and also thank the NSF CIAN ERC (Grant EEC-0812072).

References

1. V. R. Almeida, C. A. Barrios, R. R. Panepucci, and M. Lipson, Nature **431**, 1081 (2004).
2. M. Hochberg, T. Baehr-Jones, G. Wang, M. Shearn, K. Harvard, J. Luo, B. Chen, Z. Shi, R. Lawson, P. Sullivan, A. K. Y. Jen, L. Dalton, and A. Scherer, Nature Mater. **5**, 703 (2006).
3. C. Reimer, M. Kues, L. Caspani, B. Wetzel, P. Roztocki, M. Clerici, Y. Jestin, M. Ferrera, M. Peccianti, A. Pasquazi, B. E. Little, S. T. Chu, D. J. Moss, and R. Morandotti, Nature Commun. **6**, 8236 (2015).
4. M. Pöllinger and A. Rauschenbeutel, Opt. Express **18**, 17764 (2010).
5. D. T. H. Tan, P. C. Sun, and Y. Fainman, Nature Commun. **1**, 116 (2010).
6. S. Lan, L. Kang, D. T. Schoen, S. P. Rodrigues, Y. Cui, M. L. Brongersma, and W. Cai, Nature Mater. **14**, 807 (2015).
7. T. Volz, A. Reinhard, M. Winger, A. Badolato, K. J. Hennessy, E. L. Lu, and A. Imamoğlu, Nature Photon. **6**, 605 (2012).
8. D. Englund, A. Majumdar, M. Bajcsy, A. Faraon, P. Petroff, and J. Vučković, Phys. Rev. Lett. **108**, 093604 (2012).
9. J. Zhang, K. F. MacDonald, and N. I. Zheludev, Light Sci. Appl. **1**, e18 (2012).
10. X. Fang, K. F. MacDonald, and N. I. Zheludev, Light Sci. Appl. **4**, e292 (2015).
11. Y. D. Chong, L. Ge, H. Cao, and A. D. Stone, Phys. Rev. Lett. **105**, 053901 (2010).
12. W. Wan, Y. D. Chong, L. Ge, H. Noh, A. D. Stone, and H. Cao, Science **331**, 889 (2011).
13. Y. D. Chong, L. Ge, and A. D. Stone, Phys. Rev. Lett. **106**, 93902 (2011).
14. Y. Sun, W. Tan, H. Li, J. Li, and H. Chen, Phys. Rev. Lett. **112**, 143903 (2014).
15. K. G. Makris, R. El-Ganainy, D. N. Christodoulides, and Z. H. Musslimani, Phys. Rev. Lett. **100**, 103904 (2008).
16. S. Longhi and G. Della Valle, Phys. Rev. A **85**, 012112 (2012).
17. A. Mostafazadeh, Phys. Rev. Lett. **102**, 220402 (2009).
18. C. E. Rüter, K. G. Makris, R. El-Ganainy, D. N. Christodoulides, M. Segev, and D. Kip, Nature Phys. **6**, 192 (2010).
19. A. Guo, G. J. Salamo, D. Duchesne, R. Morandotti, M. Volatier-Ravat, V. Aimez, G.

A. Siviloglou, and D. N. Christodoulides, Phys. Rev. Lett. **103,** 093902 (2009).
20. L. Ge and A. D. Stone, Phys. Rev. X **4**, 031011 (2014).
21. S. Longhi, Phys. Rev. A **82** 031801(R) (2010).
22. L. Feng, Z. J. Wong, R.-M. Ma, Y. Wang, and X. Zhang, Science **346**, 972 (2014).
23. H. Hodaei, M. A. Miri, M. Heinrich, D. N. Christodoulides, and M. Khajavikhan, Science **346**, 975 (2014).
24. M. Brandstetter, M. Liertzer, C. Deutsch, P. Klang, J. Schöberl, H. E. Türeci, G. Strasser, K. Unterrainer, and S. Rotter, Nature Commun. **5**, 4034 (2014).
25. B. Peng, Ş. K. Özdemir, S, Rotter, H. Yilmaz, M. Liertzer, F. Monifi, C. M. Bender, F. Nori, and L. Yang, Science **346**, 328 (2014).
26. R. El-Ganainy, M. Khajavikhan, and L. Ge, Phys. Rev. A **90**, 013802 (2014).
27. Z. Lin, H. Ramezani, T. Eichlkraut, T. Kottos, H. Cao, and D. N. Christodoulides, Phys. Rev. Lett. **106**, 213901 (2011).
28. A. Regensburger, C. Bersch, M. -A. Miri, G. Onishchukov, D. N. Christodoulides, and U. Peschel, Nature **488,** 167 (2012).
29. L. Feng, Y. –L. Xu, W. S. Fegadolli, M. –H. Lu, J. E. B. Oliveira, V. R. Almeida, Y, -F. Chen, and A. Scherer, Nature Mater. **12**, 108 (2013).
30. L. Ge, Y. D. Chong, and A. D. Stone, Phys. Rev. A **85**, 023802 (2012).
31. B. Peng, Ş. K. Özdemir, F. Lei, F. Monifi, M. Gianfreda, G. L. Long, S. Fan, F. Nori, C. M. Bender, and L. Yang, Nature Phys. **10**, 394 (2014).
32. L. Chang, X. Jiang, S. Hua, C. Yang, J. Wen, L. Jiang, G. Li, G. Wang, and M. Xiao, Nature Photon. **8**, 524 (2014).
33. See Supplementary Material.
34. A. A. Zyablovsky, A. P. Vinogradov, A. A. Pukhov, A. V. Dorofeenko, and A. A. Lisyansky, Phys. Usp. **57**, 1063 (2014).
35. Y. Shi, Z. Yu, and S. Fan, Nature Photon. **9**, 388 (2015).
36. S. V. Suchkov, A. A. Sukhorukov, J. Huang, S. V. Dmitriev, C. Lee, and Y. S. Kivshar, Laser Photon. Rev. **10**, 177 (2016).
37. Y. Lumer, Y. Plotnik, M. C. Rechtsman, and M. Segev, Phy. Rev. Lett. **111**, 263901 (2013).
38. Y. Cui, K. H. Fung, J. Xu, H. Ma, Y. Jin, S. He, and N. Fang, Nano Lett. **12** 1443

(2010).

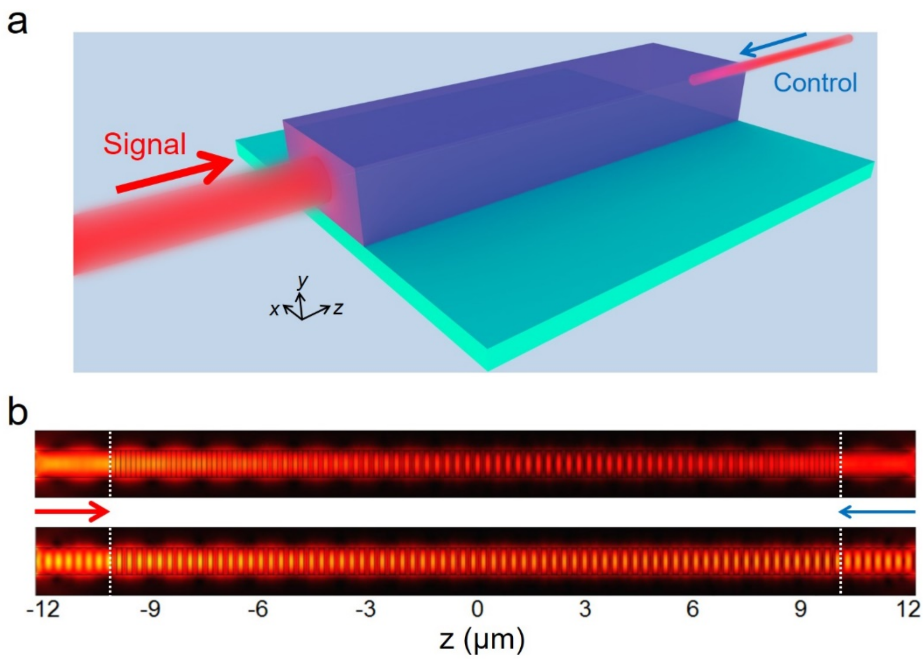

FIG. 1. Asymmetric interferometric light-light switching: (a) Schematic of a metawaveguide with asymmetric reflection, i.e. $|r_L| \neq |r_R|$. The intrinsic reflection asymmetry in the vicinity of the quasi-PT exceptional point facilitates asymmetric interferometric light-light switching of a strong source signal (forward input) by a weak control field (backward input). (b) Electric field distributions of interferometically controlled asymmetric light-light switching, where the power ratio of the weak control to the strong source signal is set to 1:3. If the incidenct phase of the control is $\varphi = \pi/2$ (upper panel), the CPA mode is achieved with no scattering, validated by the vanishing of interference patterns between inputs and outputs in both ports outside the modulation region; whereas if the incident phase of the control is $\varphi = -\pi/2$ (lower panel), the degenerated mode of less absorption is demonstrated, leading to strong output scatterings in both ports that can be seen by the interference patterns outside the modulation region.

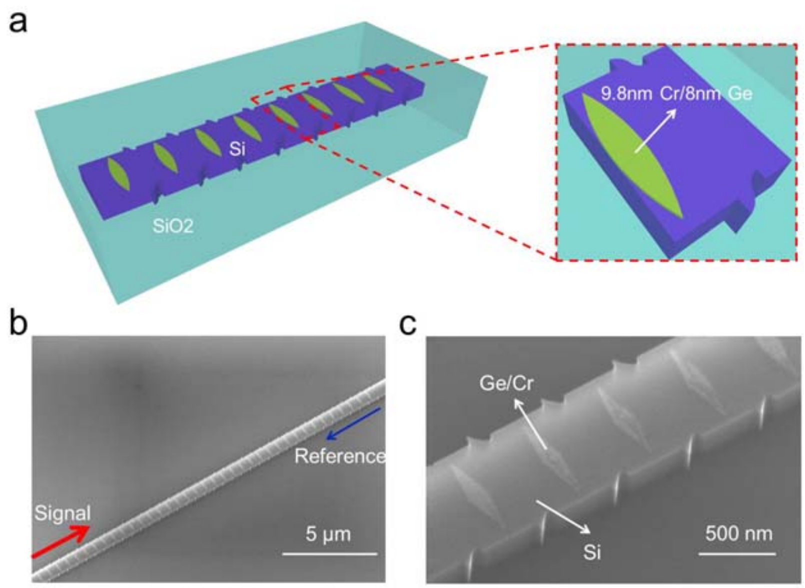

FIG. 2. Metawaveguide for asymmetric interferometric light-light switching: (a) Design of the non-Hermitian metawaveguide to create a spatial modulation equivalent to that in Eq. (2): The real index modulations of are shifted $2\pi/q$ along the length of the waveguide and emulated using side wall modulations with a transverse modulation depth cosine-varying from +71 nm to -48.5nm; the imaginary absorption modulations remain unchanged at their original locations, mimicked using bilayer sinusoidal shaped combo structures of 9.8 nm chrome (Cr)/ 8nm germanium (Ge) deposited on top of the Si waveguide. (b) SEM picture of the device consisting of 38 periods for strong signal light switching by a weak control. (c) Zoom-in picture of the metawaveguide. The profile of waveguide side wall along with Ge/Cr combo structures on top respectively realizes the designed real and imaginary modulation.

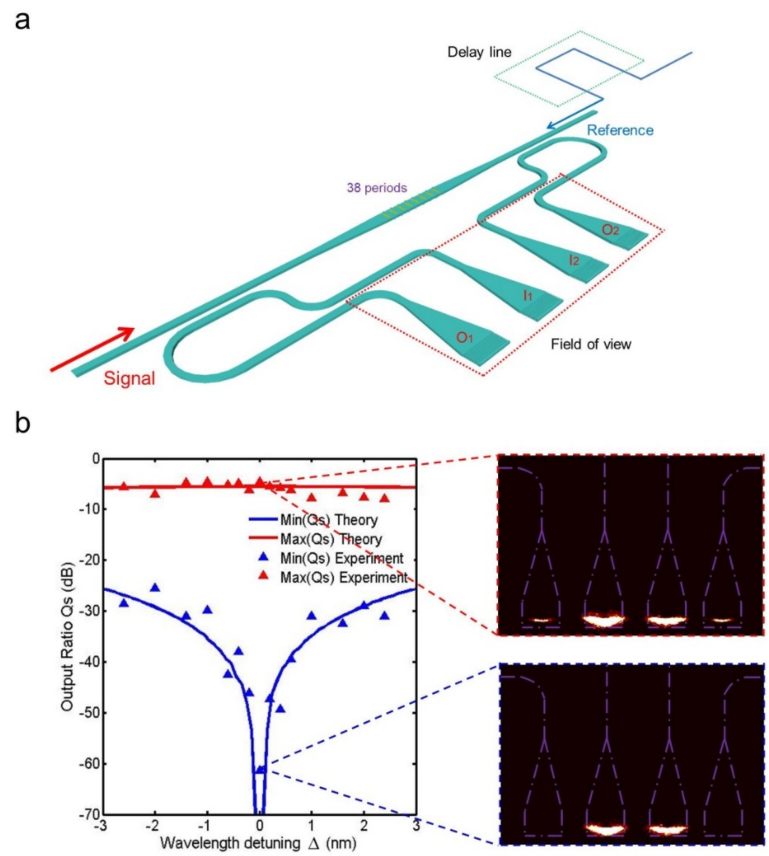

FIG. 3. Characterization of asymmetric interferometric light-light switching: (a) Configuration of the experiment setup. (b) Spectra of maximum (red) and minimum (blue) output scattering coefficients as a function of wavelength detuning (Δ) to the resonant waveglength. Insets: microscope snapshots of the scattering (top) and CPA (bottom) modes at the resonance under an exposure time of 15 ms. While the designd resonance is located at 1550 nm, the measurement results show a resonant wavelength of approximately 1540 nm. The overall detection loss due to the light splitting at the directional coupler is estimated to be 6 dB at 1540 nm. Nevertheless, the experimental results (triangles) of asymmetric interferometric light-light switching remains the same with respect to the wavelength detuning, showing an extinceion ratio of approxmiately 60 dB at the resonance.

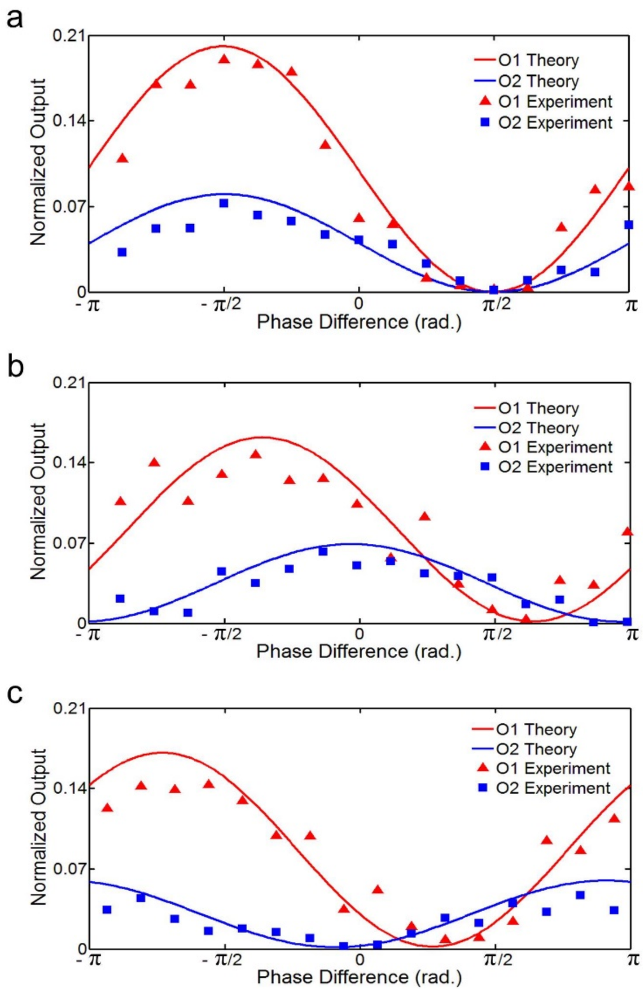

FIG. 4. Phase responses of outputs in interferometric light-light switching. (a) When operated at the resonance wavelength, two outputs oscillate in phase and reach their minimum simultaneously at $\varphi = \pi/2$, where almost no light is scattered from the two grating couplers of outputs. As the phase difference is flipped to $\varphi = -\pi/2$, peak output scattering is obtained from both grating couplers. (b) When operated at off-resonance wavelength $\Delta = -4.2$ nm, due to extra phase shift, the two output oscillations move forward. Since the output O_2 accumulates more phase than O_1, the responses are no more in phase and thus the two outputs reach minimum or maximum asynchronously. (c) When operated at off-resonance wavelength $\Delta = 4.6$ nm, the extra phase shift changes sign and results in a shift of output oscillations in the opposite direction. Note that neither of the output power can be completely eliminated at $\Delta \neq 0$ regardless of the phase tuning. The output power is normalized to the total incident power I_1+I_2 in the plots.